Science Advances
AAAS

Supplementary Materials for

Nutrients and pheromones promote insulin release to inhibit courtship drive

Liwei Zhang*, Xuan Guo, Wei Zhang*

*Corresponding author. Email: wei_zhang@mail.tsinghua.edu.cn (W.Z.); lwzhang@cau.edu.cn (L.Z.)

Published 9 March 2022, *Sci. Adv.* **8**, eabl6121 (2022)
DOI: 10.1126/sciadv.abl6121

This PDF file includes:

Supplementary figures and table

Fig. S1

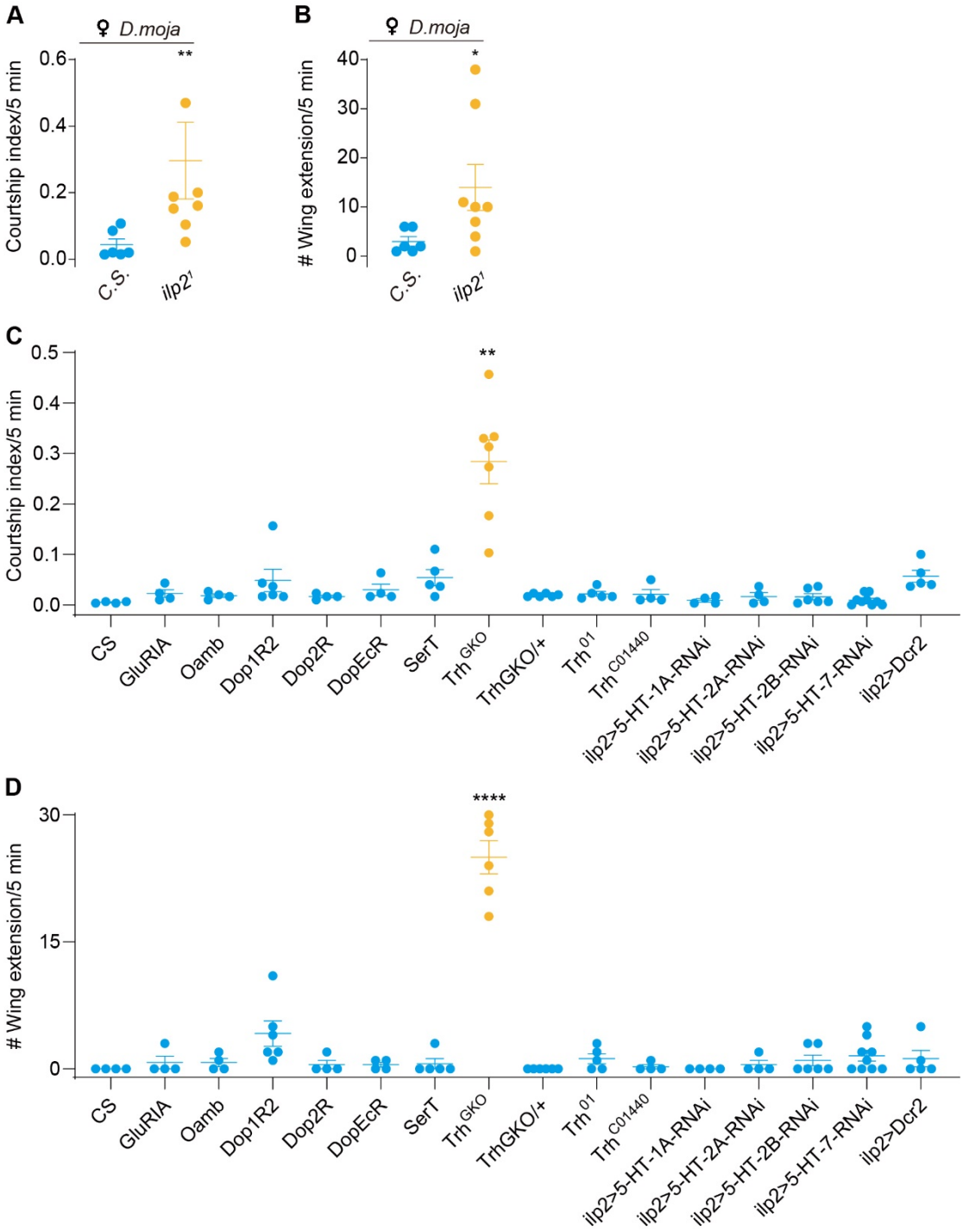

Fig. S1. Screening for neurotransmitter genes involved in inter-male courtship. (**A** and **B**) *ilp2*^{1} mutant males exhibited increased courtship activity towards *D.mojavensis* virgin females. Courtship index and single-wing extension number were quantified in CS and *ilp2*^{1} mutant males. N=6-7 for each genotype. Mann-Whitney nonparametric test was used. **p < 0.01, *p < 0.05. Data were represented as mean ± SEM. (**C** and **D**) No inter-male courtship was observed in the mutants of neurotransmitter or receptor genes except for the *Trh*^{GKO} mutant males. Knocking down serotonin receptors in IPCs displayed no inter-male courtship. Courtship index (A) and single-wing extension

number (B) between males with indicated genotypes. N=4-7 in each group. One-way ANOVA followed with Dunnett test for multiple comparisons was used and statistical differences were represented as following: **p < 0.01, ****p < 0.0001. Data were represented as mean ± SEM.

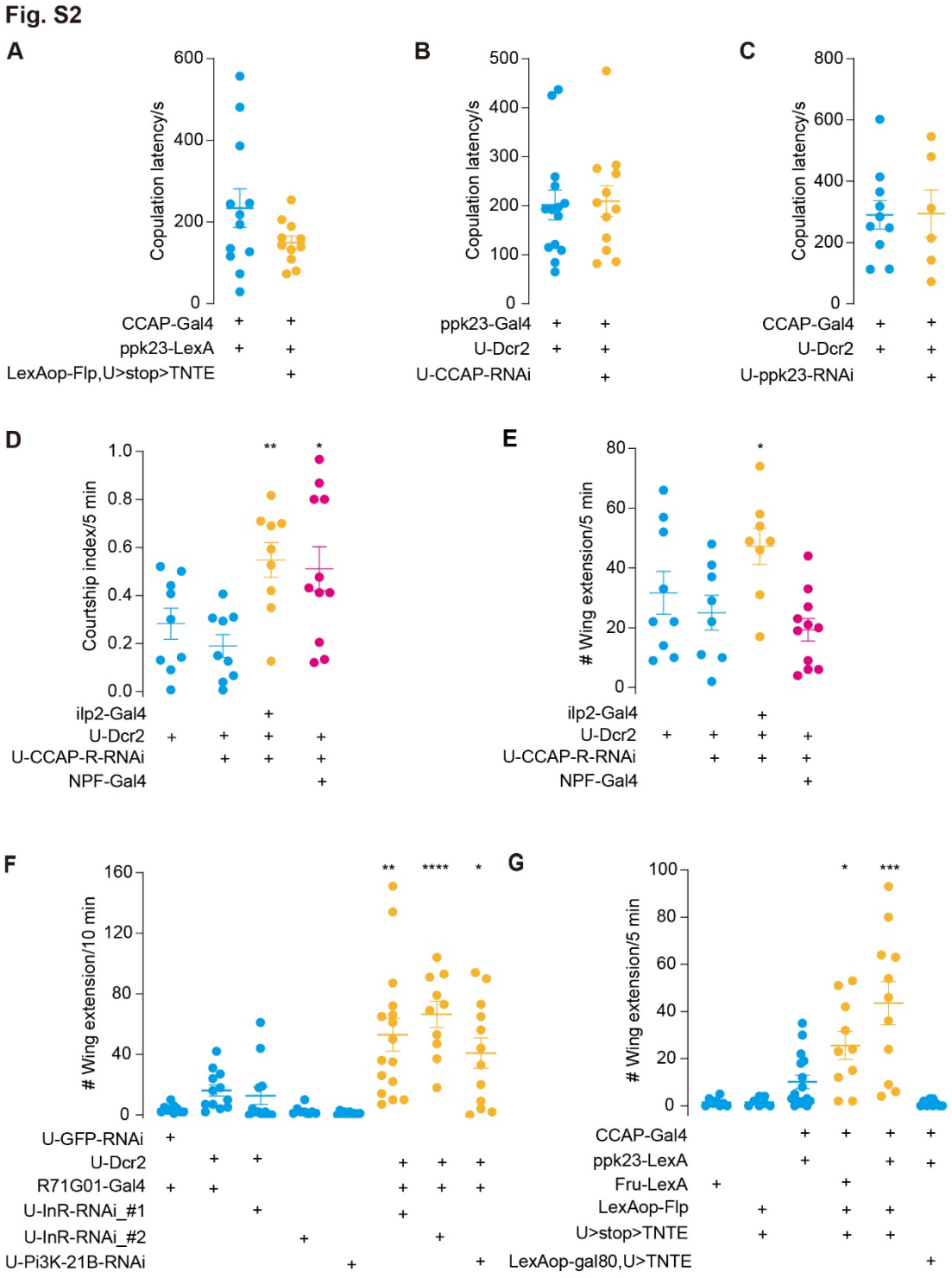

Fig. S2. Knockdown CCAP or silencing CCAP/PPK23 co-labeled neurons didn't affect male-female courtship. (**A** to **C**) Courtship activity between pairs of indicated males and w^{1118} virgin female. None of silencing CCAP/PPK23 neurons in (A), suppressing CCAP expression by PPK23-Gal4 in (B) or suppressing ppk23 expression by CCAP-Gal4 in (C) disrupted male-female courtship.

N =11-12 in each group of (A), n=12-14 in each group of (B) and n=6-10 in each group of (C). Mann-Whitney nonparametric tests were used. Data were represented as mean ± SEM. (**D** and **E**) Courtship index and single-wing extension number in indicated groups. One-way ANOVA nonparametric Kruskal-Wallis tests followed with Dunn's test compared with U-Dcr2; U-CCAP-R-RNAi group were used. Data were represented as mean ± SEM. N=7-12 in each group. *p < 0.05, ***p < 0.001. (**F**) Single-wing extension numbers in indicated groups when InR signaling in P1 neurons were disrupted. N=7-12 in each group. One-way ANOVA nonparametric Kruskal-Wallis tests followed with Dunn's test compared with R71G01-Gal4 were used. Data were represented as mean ± SEM. *p < 0.05, **p < 0.01, ****p < 0.0001. (**G**) Single-wing extension numbers in indicated groups when ppk23/CCAP neurons were silenced. N=7-11 in each group. One-way ANOVA nonparametric Kruskal-Wallis tests followed with Dunn's test compared with Fru-LexA was used. Data were represented as mean ± SEM. *p < 0.05, **#p < 0.001.

Fig. S3

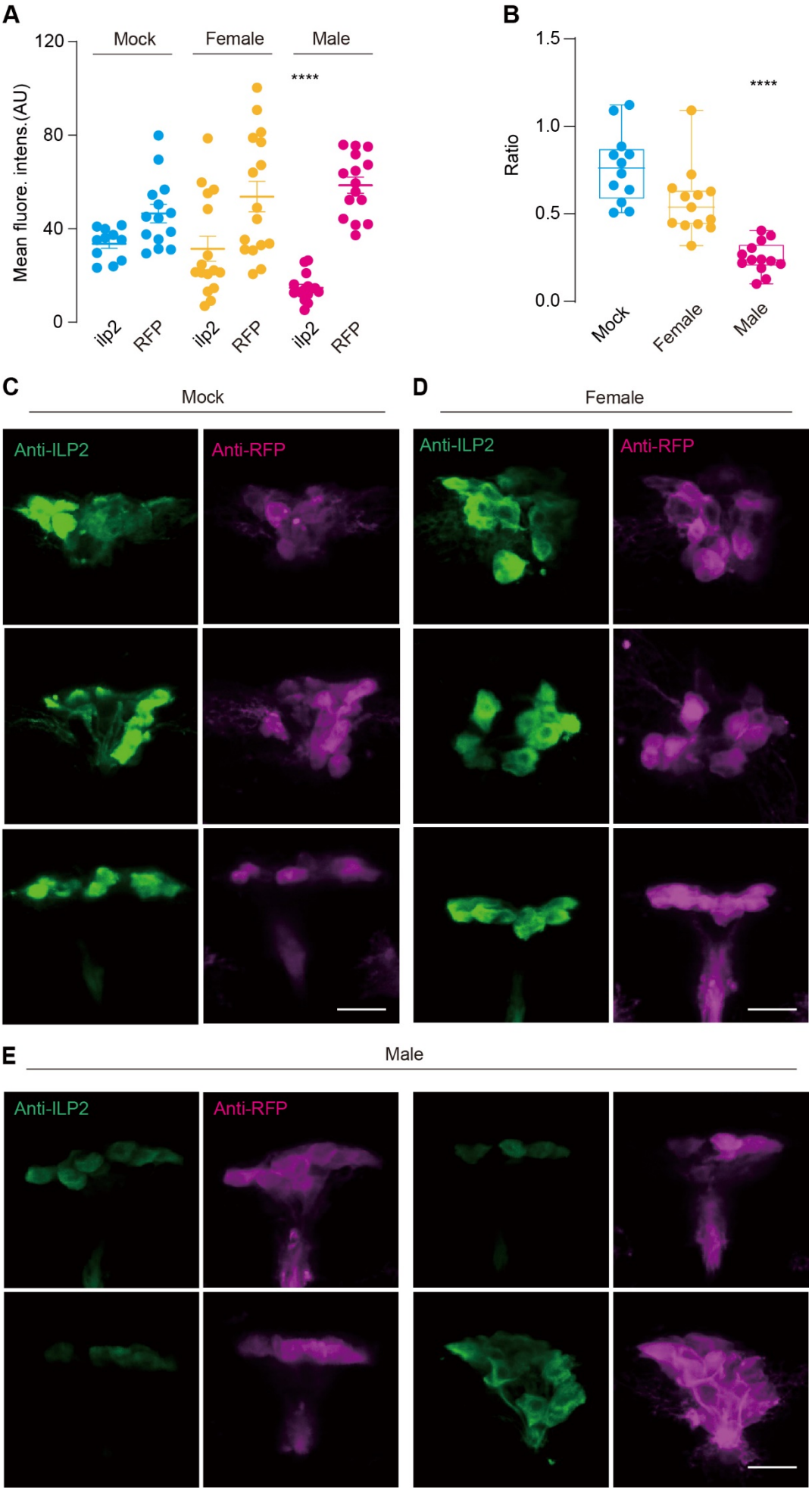
A
Mock
Female
Male
120
80
40
0
Mean fluore. intens.(AU)
****
ilp2
RFP
ilp2
RFP
ilp2
RFP
B
1.5
1.0
0.5
0.0
Ratio
****
Mock
Female
Male
C
Mock
Anti-ILP2
Anti-RFP
D
Female
Anti-ILP2
Anti-RFP
E
Male
Anti-ILP2
Anti-RFP

Fig. S3. Quantification of ILP2 release in IPCs. (**A**) Mean fluorescence intensities in IPCs stained with ILP2 and RFP antibodies respectively. In two adjacent groups, A.U. values between anti-ILP2 and anti-RFP were compared. Males (ilp2-LexA/+; lexAop-mCD2-RFP/+) were grouped with conspecific female and male, as well as mock control. Mann-Whitney nonparametric tests were used in each treatment. Data were represented as mean ± SEM. ****$p < 0.0001$. (**B**) A.U. value ratios (anti-ILP2 divided by anti-RFP) were quantified between genotypes in (A). One-way ANOVA nonparametric Kruskal-Wallis tests followed with Dunn's test compared with mock group were used. Data were represented as mean ± SEM. ****$p < 0.0001$. (**C**-**E**) More image samples from three groups in (A). Bar: 20μm.

Fig. S4

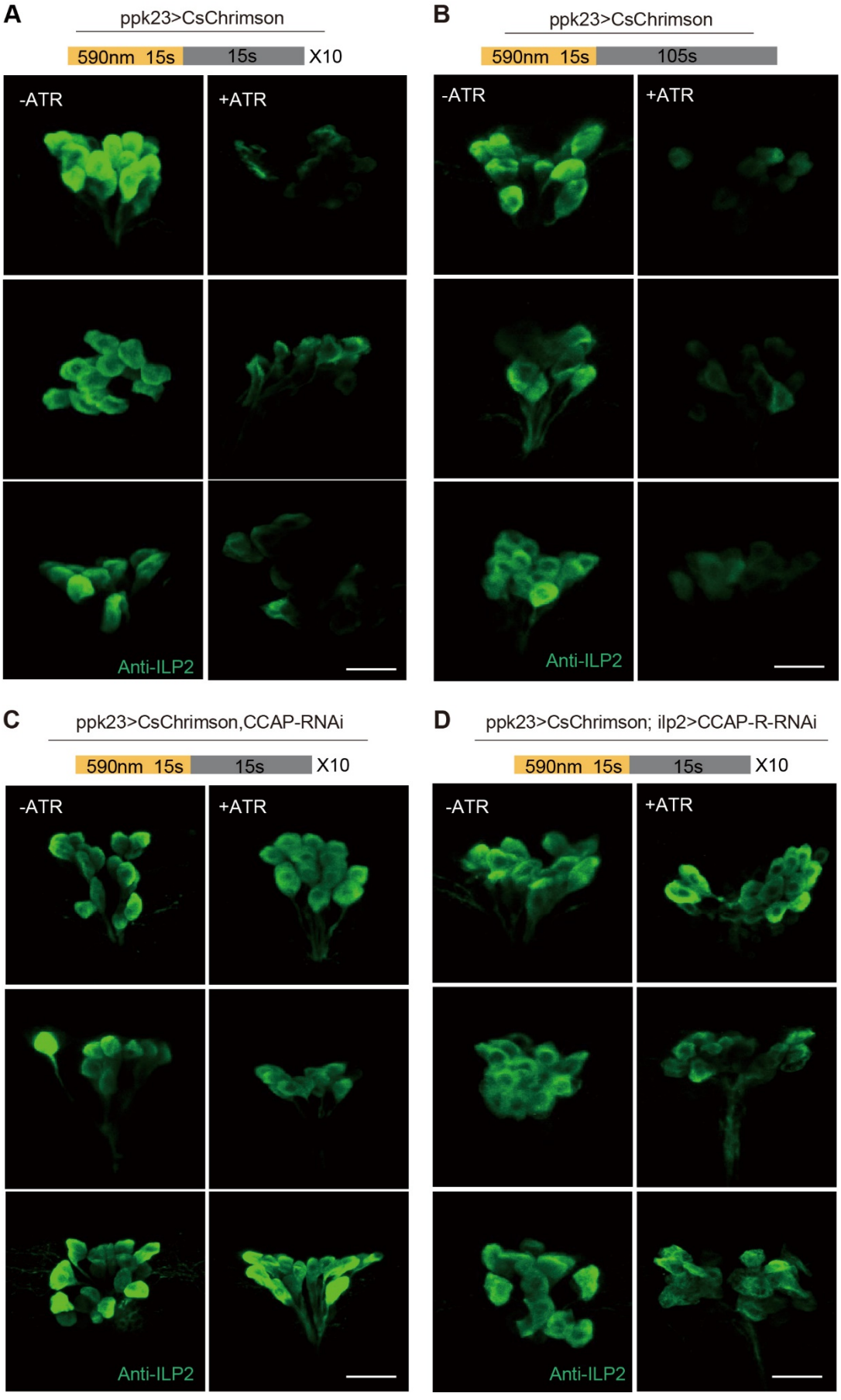
A
ppk23>CsChrimson
590nm 15s
15s
X10
-ATR
+ATR
Anti-ILP2
B
ppk23>CsChrimson
590nm 15s
105s
-ATR
+ATR
Anti-ILP2
C
ppk23>CsChrimson,CCAP-RNAi
590nm 15s
15s
X10
-ATR
+ATR
Anti-ILP2
D
ppk23>CsChrimson; ilp2>CCAP-R-RNAi
590nm 15s
15s
X10
-ATR
+ATR
Anti-ILP2

Fig. S4. Image samples of ILP2 immunostainings in various manipulations. (**A** to **D**) IPCs immunostaining intensities after optogenetic activation of ppk23+ cells (A and B), coupled with CCAP-RNAi in ppk23+ cells (C) or coupled with CCAP-R-RNAi in IPCs (D). Bar: 20μm.

Fig. S5

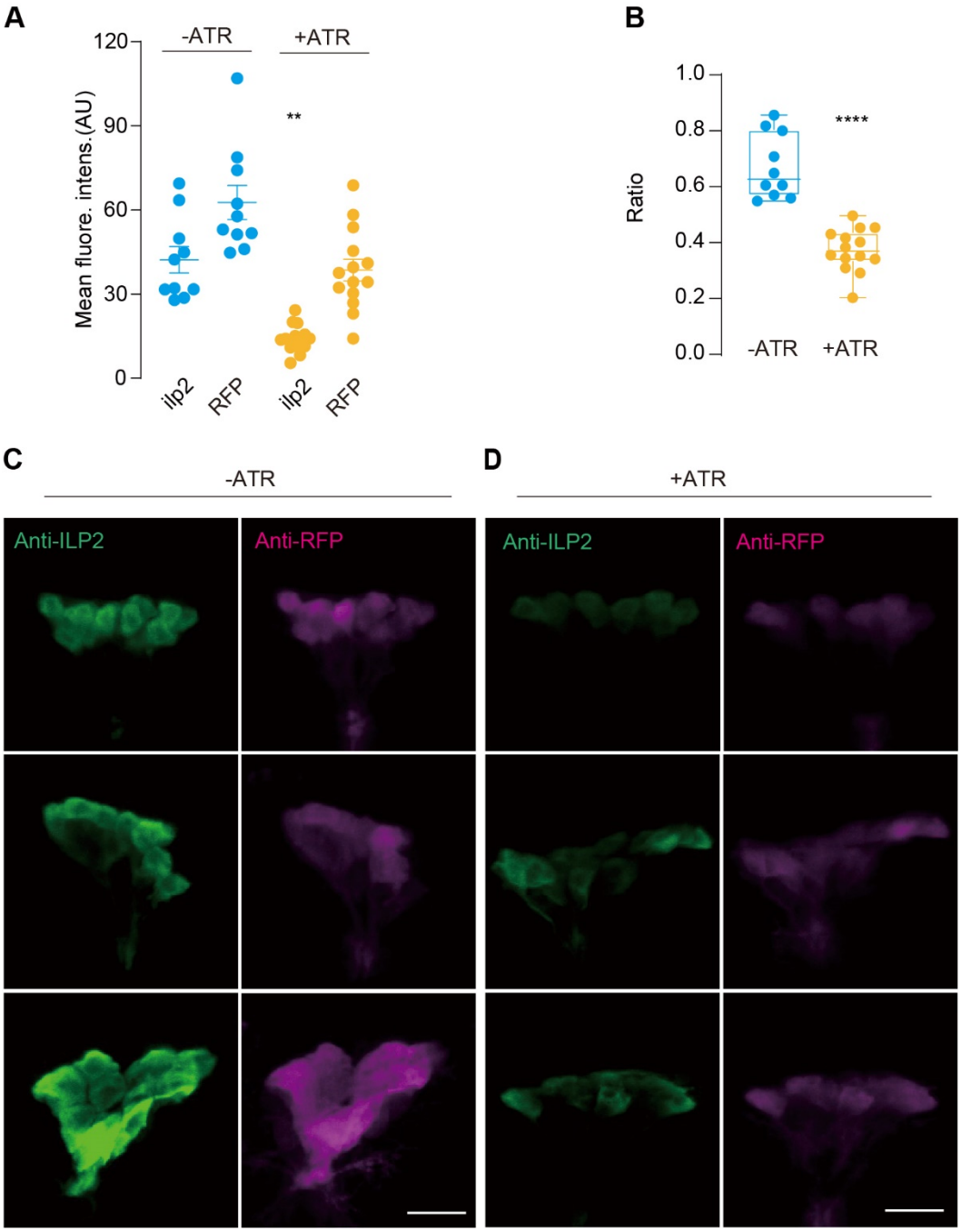

Fig. S5. Quantification of ILP2 level under optogenetic manipulations. (**A**) Mean fluorescence intensity (A.U.) of ILP2 and RFP when supplied with all-trans retinal (+ATR) or not (-ATR) in males (UAS-CsChrimson/ilp2-lexA; LexAop-mCD2-RFP/ppk23-gal4). Related to Fig. 5G. The diminishment of RFP intensity in +ATR treatment might be from either accompanying release with DILPs or reduced transcript level of RFP during the long-term activation of IPCs. (**B**) Normalization (ratio) of ILP2 immuno-intensity with respect to RFP level with all-trans retinal (+ATR) or not (-

ATR) in males (UAS-CsChrimson/ilp2-lex; LexAop-RFP/ppk23-gal4) related to (A). (**C** and **D**) More image samples from two groups in (A). Bar: 20μm.

Fig. S6

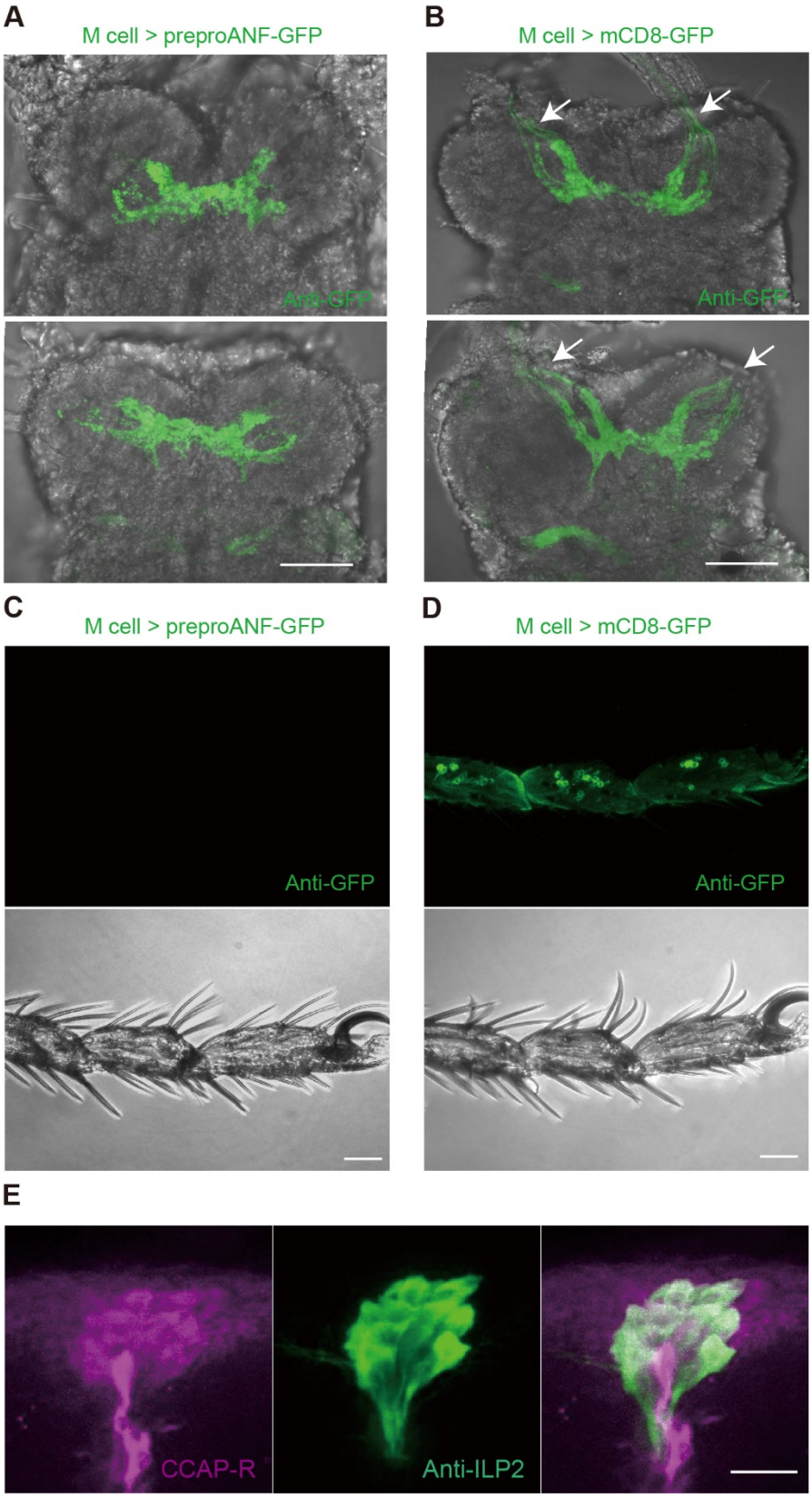

Fig. S6. Dense core vesicles localizations in ppk23+/CCAP+ cells axon and expression of CCAP-R on IPCs. (**A**) Visualization of dense core vesicles in M-cells' (vGlut-Gal80; ppk23-Gal4) axonal projections in the VNC. Anti-GFP signals were observed in males of ppk23-Gal4>UAS-preproANF-Emerald. No staining signal was observed outside the VNC, indicating that neuropeptides were released within the VNC. Bar: 20μm. (**B**) Visualization of axonal projections of M-cells (vGlut-Gal80; ppk23-Gal4) in the VNC. Anti-GFP signals were observed in males of ppk23-Gal4>UAS-mCD8-GFP. White arrow indicated the fiber bundles that enter the VNC from leg ppk23+ neurons. Bar: 20 μm. (**C**) No dense core vesicles signal was found on male legs (vGlut-Gal80; ppk23-Gal4>UAS-preproANF-Emerald). Bar: 20 μm. (**D**) ppk23+ neurons were found on male legs with GFP (vGlut-Gal80; ppk23-Gal4>UAS-mCD8-GFP). Bar: 20 μm. (**E**) Co-localization between CCAP-R+ neurons (R64B05-Gal4>GFP) and IPCs (anti-ILP2). Bar: 20 μm.

Fig. S7

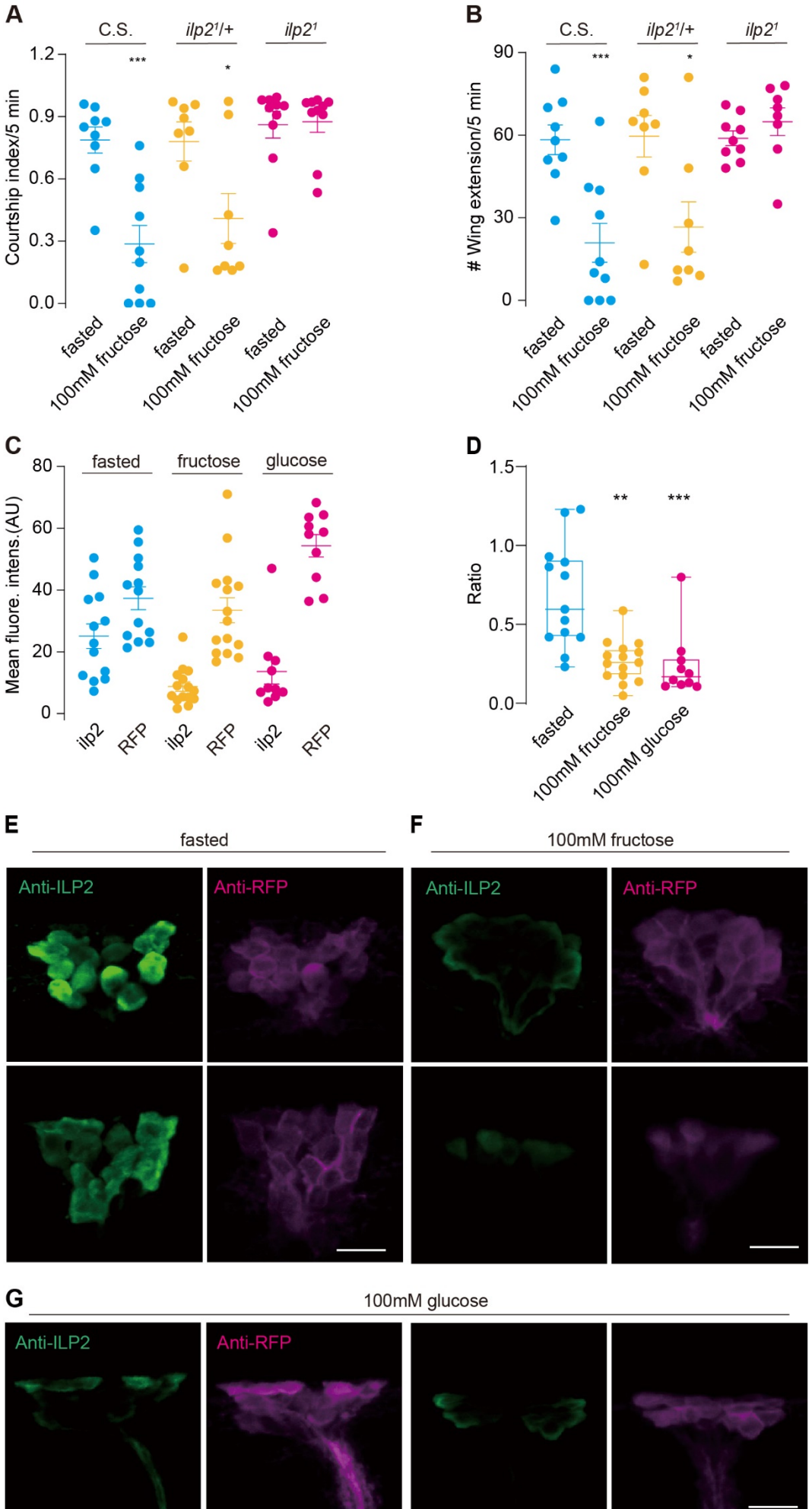
A
C.S.
ilp2¹/+
ilp2¹
Courtship index/5 min
1.2
0.9
0.6
0.3
0.0
***
*
fasted
100mM fructose
B
Wing extension/5 min
90
60
30
0
C
fasted
fructose
glucose
Mean fluore. intens.(AU)
80
60
40
20
0
ilp2
RFP
D
Ratio
1.5
1.0
0.5
0.0
**
***
100mM glucose
E
F
G
Anti-ILP2
Anti-RFP

Fig. S7. Effects of sugar meal on courtship in fasted males. (**A** and **B**) Courtship and single-wing extension number in CS, *ilp2*^{1} heterozygous and *ilp2*^{1} homozygous mutant males toward w^{1118} virgin females. All males were starved for 16 hours during which water was supplied, and then fed with 100 mM fructose for 3 min before test. Mann-Whitney nonparametric test was used in two groups of the same genotypes. *p < 0.05, ***p < 0.001. Data were represented as mean ± SEM. (**C**) Mean fluorescence intensity (A.U.) of ILP2 and RFP in fasted, fructose- or glucose-fed males related to Fig. 3**A-B**. (**D**) Normalization (ratio) of ILP2 immuno-intensity with respect to RFP level in fasted, fructose- or glucose-fed males related to (C). One-way ANOVA nonparametric Kruskal-Wallis tests followed with Dunn's test compared with fasted group were used. Data were represented as mean ± SEM. **p < 0.01, ***p < 0.001. (**E** to **G**) Representative samples from three groups in (C). Bar: 20 μm.

Fig. S8

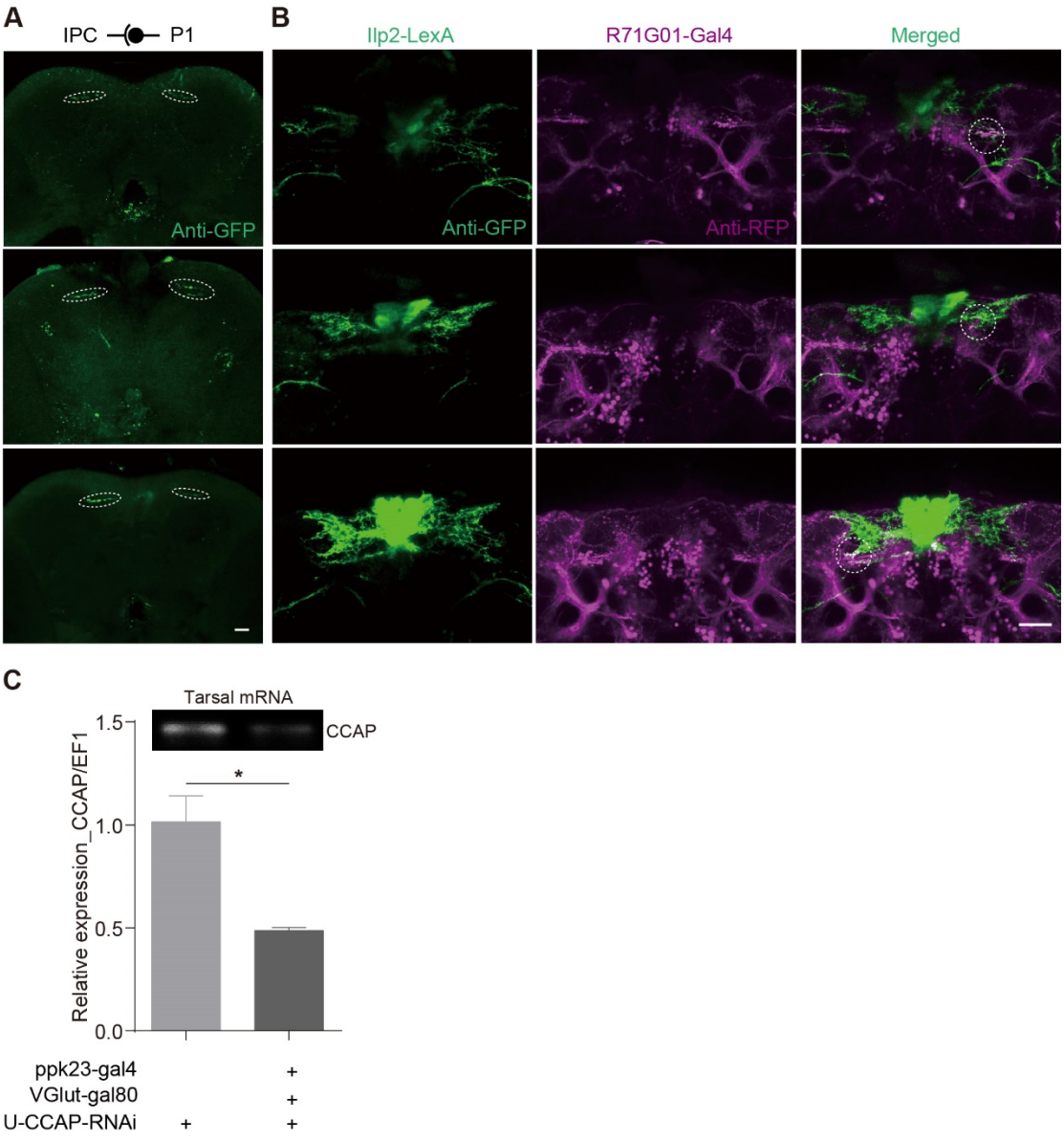

Fig. S8. Putative connections between IPCs and P1 neurons and CCAP expression in M-cells. (**A**) GRASP signals were detected between IPCs and P1 neurons. Genotype: ilp2-LexA/+; UAS-

CD4-spGFP1-10, LexAop-CD4-spGFP11/R71G01-Gal4. Dotted circles indicated the GRASP signals. Bar: 20 μm. (**B**) Spatial relation between IPCs and P1 neurons. Genotype: ilp2-LexA/UAS-tdTomato; LexAop-mCD8-GFP/R71G01-Gal4. Dotted circles indicated the adjacent regions where IPCs and P1 neurons are in close proximity. Bar: 20 μm. (**C**) Q-PCR quantification of leg tarsal CCAP transcripts. Top gel image was correlated with column below. UAS-CCAP-RNAi males were used as control and vGlut-Gal80; ppk23-Gal4>UAS-CCAP-RNAi males were treatment group. Mann-Whitney nonparametric test was used for statistical analysis. N=3 for each group. *$p < 0.05$. Data were represented as mean ± SEM.

Table. S1. RNAi lines and mutant alleles used in screening.

Lines used in Figure 3.		**Lines used in Figure S1.**	
Gene/Allele	**BDSC #**	**Gene/Allele**	**BDSC #**
Dromyosuppressin R	25832	$GluRIA^{attP}$	84506
Fmrf R	25858	$Oamb^{del}$	84707
Diuretic hormone 31 R1	25925	$Dop1R2^{KO}$	84719
Allatostatin R2	25935	$Dop2R^{KO}$	84720
Leucokinin R	25936	$DopEcR^{KOGal4}$	84717
NPF R	25939	$SerT^{attP}$	84572
Capa R	27275	Trh^{GKO}	86146
Allatostatin R	27280	Trh^{01}	86147
CCK like R	27494	Trh^{c01440}	10531
CCHamide-1 R	27669	UAS-5-HT1A-$IR^{JF01852}$	25834
Allatostatin C R1	27506	UAS-5-HT2A-$IR^{JF02157}$	31882
short NPF R	27507	UAS-5-HT1B-$IR^{JF01851}$	25833
Fsh-Tsh-Like R	27509		
Tachykinin-like R at 99D	27513		
Dromyosuppressin R1	27529		
Pyrokinin 1 R	27539		
Eclosion hormone R	38346		
Diuretic hormone 44 R1	28780		
Pyrokinin 2 R2	28781		
ETH R	28783		
Proctolin R	29414		
AKH R	29577		
Pyrokinin 2 R1	29624		
Cardioacceleratory peptide R (CCAP R)	31490		
SIFamide R	34947		

Tachykinin like R at 86C	31884		
Bursicon R	31958		
Pdf R	38347		